Published in final edited form as:
NMR Biomed. 2011 October ; 24(8): 1023–1028. doi:10.1002/nbm.1717.

PHIP Hyperpolarized MR Receptor Imaging *In Vivo*: A Pilot Study of ^{13}C Imaging of Atheroma in Mice

Pratip Bhattacharya[1,§], **Eduard Y. Chekmenev**[1,2], **Wanda F. Reynolds**[3], **Shawn R. Wagner**[1], **Niki Zacharias**[1], **Henry R. Chan**[1], **Rolf Bünger**[4], and **Brian D. Ross**[1]

[1]Enhanced Magnetic Resonance Laboratory, Huntington Medical Research Institutes, Pasadena, CA 91105

[2]Rudi Schulte Research Institute, Santa Barbara, CA

[3]Sanford Burnham Medical Research Institute, La Jolla, CA

[4]Uniformed Services University of the Health Sciences, Bethesda, MD 20814

Abstract

Background—Magnetic resonance (MR) techniques using hyperpolarized ^{13}C have successfully produced examples of angiography and intermediary metabolic imaging, but to date no receptor imaging has been attempted. The goal of this study is to synthesize and evaluate a novel hyperpolarizable molecule, tetrafluoropropyl 1-^{13}C-propionate-d3 (TFPP), for detecting atheromatous plaque *in vivo*. TFPP binds to lipid bilayers and its use in hyperpolarized MR could prove to be a major step towards receptor imaging.

Results—The precursor, Tetrafluoropropyl 1-^{13}C-acrylate (TFPA) binds to dimyristoylphosphatidylcholine (DMPC) lipid bilayers with a 1.6 ppm chemical shift in the ^{19}F MR spectrum. This molecule was designed to be hyperpolarized through addition of parahydrogen to ^{13}C acrylate moiety by Parahydrogen Induced Polarization (PHIP). ^{13}C TFPA was hyperpolarized to Tetrafluoropropyl 1-^{13}C-propionate (TFPP) to a similar extent to that of hydroxyethylacrylate (HEA) to hydroxyethylpropionate (HEP); 17% +/− 4 % for TFPP vs 20% for HEP; T_1 relaxation times (45s ± 2 vs 55s ± 2) were comparable and the hyperpolarized properties of TFPP were characterized. HEA, like TFPA has a chemical structure with an acrylate moiety but do not have the lipid binding Tetrafluoropropyl functional group. Hyperpolarized ^{13}C TFPP binds to lipid bilayer appearing as a second, chemically shifted ^{13}C hyperpolarized MR resonance with further reduction in longitudinal relaxation time (T_1 = 21s ± 1). In aortas harvested from Low Density Lipoprotein Receptor (LDLR) knock-out mice fed with a high fat diet for nine months, and in which atheroma is deposited in aorta and heart, ^{13}C TFPP showed greater binding to lipid on the intimal surface than in normal diet control mice. When ^{13}C TFPP was hyperpolarized and administered *in vivo* to atheromatous mice in a pilot study, increased binding was observed on the endocardial surface of the intact heart compared to normal fed controls.

Conclusions—Hyperpolarized ^{13}C TFPP has bio-sensing specificity for lipid, coupled with 42,000 fold sensitivity gain in MR signal at 4.7 Tesla. Binding of TFPP with lipids results in the formation of a characteristic second peak in MR spectroscopy. TFPP therefore has the potential to act as an *in vivo* molecular probe for atheromatous plaque imaging and may serve as a model of receptor targeted bioimaging with enhanced MR sensitivity.

[§]**Corresponding author:** Pratip Bhattacharya, PhD Enhanced Magnetic Resonance Laboratory, Huntington Medical Research Institutes, 10 Pico Street Pasadena, CA 91105 pratip@hmri.org Phone: +1-626-397-5840 Fax: +1-626-397-5846.

Keywords

^{13}C; heart; receptor imaging; atheroma; hyperpolarization; TFPP; PHIP; MR

Background

Magnetic Resonance Imaging (MRI) can non-invasively measure cardiac energetics and has had an important impact on the diagnosis and understanding of cardiac function and disorders (1). The early promise of MR Spectroscopy (MRS), as a means of defining normal and disordered cardiac metabolism has not been fully realized. Current practical problems due to low sensitivity and high costs of traditional MR imaging hinder large scale applications of this technology in both basic and clinical sciences. The MR signal intensity is a function of the product of the number of spins and the fractional nuclear spin polarization; the latter is only 10^{-6}–10^{-5} for typical high field equilibrium initial conditions. This severely limits the utility of MR imaging and spectroscopy in biomedical diagnosis and research, especially for nuclei such as ^{13}C and ^{15}N. Conventional MR is simply not sensitive enough – polarization is only a few parts per million, which translates into a relatively a small number of nuclear `spins' available for image reconstruction. The difference in the spin population is proportional to the magnetic field strength, so that 3T `buys' twice the signal available at 1.5T and so on. Conventional MR is also too slow – an examination may take 30 minutes or more. At relatively low cost, hyperpolarization has the potential of solving many of these problems by amplifying MR signal 10,000 – 100,000 fold. With this sensitivity gain, hyperpolarization may enable *in vivo* nanochemistry and metabolomics, decreases the time needed to observe a metabolite concentration change, better extracts the signal of a target molecule against a background of low spin species in a mixture, or *in vivo* (i.e.^{13}C background is only 1.1% while water protons fall to zero in a hyperpolarized ^{13}C imaging study) and permits studies to be performed faster and at considerably lower cost.

Dynamic Nuclear Polarization (DNP)(2) and Parahydrogen Induced Polarization (PHIP) (3,4) allow nuclear spin polarization to reach order of unity, where nearly all nuclear magnetic moments contribute to the MR signal. These techniques constitute the emerging field of hyperpolarization that increases signal-to-noise ratio by a factor of 10^5 at reasonable costs. This has been successfully demonstrated for ^{13}C labeled compounds with spin lattice relaxation times T_1 of tens of seconds with demonstrated sensitivity enhancements by factors of 10^4–10^5 by both DNP (5–9) and PHIP (10–12). These hyperpolarized ^{13}C MR agents allow fast *in vivo* ^{13}C imaging and spectroscopy. To date, a few biologically relevant agents have been explored including 1-^{13}C-pyruvic acid (5–8) and bicarbonate (9) by DNP and 1-^{13}C-succinic acid (10,11) by PHIP. These molecules were primarily designed to target enzymatic biochemical processes at cellular and tissue levels by providing an instantaneous snapshot of uptake and metabolism of the ^{13}C-tracer. In addition, a small number of angiographic reagents (12,13) have been designed and tested *in vivo* to provide real-time coronary angiography, catheter positioning and myocardial perfusion.

Here, we present a novel class of ^{13}C hyperpolarized “receptor imaging” molecular agents which have both enhanced MR sensitivity and a moiety capable of targeted biosensing. This is exemplified by the $–CH_2$-CF_2-CF_2H fluorocarbon group which has a lipophilic propensity in aqueous medium. This moiety facilitates chemical exchange into lipids (14) shown here to manifest as a unique ^{13}C hyperpolarized spectroscopic signature. The work described here is the first step toward designing targeted enhanced MR contrast agents and initial proof of concept *in vivo*. In particular, the lipophilic functionality presented here may potentially allow for targeting of lipid rich atherosclerotic plaque (15–17) *in vivo*.

Results and Discussion

Hyperpolarization of Tetrafluoropropyl 1-^{13}Cpropionate

The design and the selection of the marker has been described elsewhere (13,14). This new molecular agent has two important moieties: the lipophilic fluorocarbon motif –CH_2-CF_2-CF_2H (15,16) and the C=C-^{13}C functionality for ^{13}C PHIP hyperpolarization (13,14). Figure 1b demonstrates the ^{13}C spectrum of hyperpolarized TFPP, a single carbonyl resonance at 177 ppm. Analysis of the peak areas of the ^{13}C spectrum in Fig. 1b yields a $\%P_{t=0}$ (Percentage of Polarization at time 0) = 17±4 % for TFPP, which corresponds to a 42,000 ± 10,000 fold enhancement of the TFPP ^{13}C MR signal at 4.7 T.

Characterization of Hyperpolarization

The percentage of hyperpolarization in TFPP is similar to ~20% polarization previously obtained with Hydroxyethylpropionate (HEP), which has a similar PHIP hyperpolarization moiety (14). The hyperpolarized signal of TFPP like HEP, is not dependent on pH, temperature and osmolarity. In addition to a high level of hyperpolarization, the lipophilic PHIP ^{13}C reagent, TFPP, retained the important MR property of a long spin lattice relaxation time (T_1) upon substitution of the 2-hydroxyethyl group in HEP by 2,2,3,3-tetrafluoropropyl group. The spin lattice relaxation time of 45±2 s was measured using hyperpolarized material at 4.7 T with 7.5° excitation pulses. This is similar to T_1 = 55±2 s for aqueous HEP under identical conditions. When hyperpolarized TFPP is mixed with synthetic 1,2-dimyristoylphosphatidylcholine (DMPC) bilayers (Avanti Polar Lipids, Inc., Alabaster, AL), an additional ^{13}C resonance at 174 ppm is detected (Fig. 2b). This significantly broader (full width at half maximum: 2.5 ppm) and chemically shifted (by 3ppm) resonance is interpreted as the fraction of TFPP signal bound to the DMPC membranes. A similar shift was observed for TFPA detected by ^{19}F spectroscopy (14). Mixing hyperpolarized TFPP with DMPC also reduced the ^{13}C spin lattice relaxation time of hyperpolarized TFPP from 45 s to ~20 s (Fig. 2b). As TFPP is a lipophilic reagent and may be useful for distinguishing of vulnerable plaque *in vivo* by sensing chemical exchange with lipids, it was also tested for interactions with porcine blood (Sierra Medical, California) (Fig. 2c). While ^{13}C T_1 is reduced to 15 s (Fig. 2c), there is no additional ^{13}C resonance, as observed for TFPP interacting with lipid membranes (Fig. 2c). This validates the hypothesis that the second ^{13}C TFPP NMR resonance at ~174 ppm is a signature of interaction with lipids, but not with blood.

Preliminary *In Vivo and In Vitro* Studies

To study the feasibility of the model of *in vivo* lipid sensing with MR hyperpolarized reagents, we examined genetically modified mice with a deficiency in low density lipoprotein receptor (LDLR). These mice will develop massive atheroma deposits in the aorta and, tricuspid and mitral valves when placed on a nine month high fat Western diet (17,18). Wild type mice with normal LDL receptor will not develop atheroma under these conditions. Specifically, we studied the interaction of TFPP with aortas (*ex vivo*) and heart (*in vivo*) of LDLR deficient and control mice. First, the animals were injected with 1 mL (based on survival, mice tolerate i–v loading with up to 1 mL of hyperpolarized reagent unpublished) of 11–42 mM solution of hyperpolarized TFPP into the heart and then a series of ^{13}C spectra (Figs. 3g and 3h) was recorded 15±5s after injection. Representative *in vivo* ^{13}C non-localized hyperpolarized NMR spectra are shown in Fig. 3g (LDLR deficient) and Fig. 3h (control mice). A representative *in vivo* time course of signal decay after intracardiac injection of ^{13}C hyperpolarized TFPP into LDLR deficient mice is shown in Fig.4. In two out of seven experiments, one control and one LDLR deficient mouse, fast ^{13}C 2D image (Fig. 3f) were acquired prior to spectroscopic acquisition of hyperpolarized TFPP *in vivo*. The co-registration of ^{13}C images with proton images revealed that ^{13}C NMR signal

was confined to the heart region in both cases. This is consistent with the view that the detected ^{13}C NMR spectra also originated from the heart (Figs. 3g and 3h). The ratio of the hyperpolarized NMR signal from TFPP molecules bound to lipids to that in solution was markedly higher in LDLR deficient mice compared to that of controls. This result is more interesting given the fact that LDLR mice are 50% larger on average than control mice and same absolute dosage has been employed in the *in vivo* trials. This demonstrates positive correlation of the quantity of lipids in aorta and heart with the experimental hyperpolarized signal ratio of (lipid TFPP):(total TFPP). We do not have enough data to explain the dramatic loss of (lipid TFPP):(total TFPP) at high dosage of TFPP but one can speculate that the toxicity of the molecule may play a role. Detailed study of *in vivo* toxicity of TFPP is in progress in our laboratory. Moreover, non-localized proton spectra acquired over the whole body of the two types of mice confirm the presence of elevated lipid content in LDLR deficient mice compared to control mice (Figs. 3c and 3d). The *in vivo* ^{13}C T_1 of hyperpolarized TFPP varied between 14 s and 22 s which is sufficiently long for imaging and spectroscopy experiments as hyperpolarized signal persists upto 5X T_1 (i.e. ~70–110 s for TFPP). The persistence of hyperpolarized signal *in vivo* is also evident in the time course studies (Fig. 4).

Following the *in vivo* experiments, the animal aortas were harvested and washed with ice-cold, 0.9% saline solution to remove the blood from the endothelial surfaces of the vessel walls. A small piece of aorta (inset of Fig. 3e) from the animal was packed in 4 mm solid state NMR rotor and mixed with the same TFPP solution used for the *in vivo* experiments described above. We utilized ^{19}F solid state magic angle spinning (MAS) NMR spectroscopy to monitor TFPP lipid binding within aortas directly. This was markedly higher in LDLR deficient mice (Fig. 3a) compared to control mice (Fig. 3b). Thus it seemed justified to rationalize that TFPP has sufficient chemical affinity to structural atheroma lipids and can therefore undergo chemical exchange with the arterial wall. Binding with any blood constituents was minimal, since the characteristic chemical shift signature from the saline incubations was also present in our ^{19}F assays, when the blood was removed from the aorta. If these rationales are valid, our data show, ^{19}F TFPP MR is capable of sensing elevated lipid content on arterial and heart vessel walls in mice *ex vivo* (Figs. 3a and 3b).

An additional NMR resonance at 186 ppm was observed in some *in vivo* ^{13}C hyperpolarized spectra with sufficiently high signal-to-noise ratio in both LDLR and control animals. There were also two NMR resonances (177 ppm and 174 ppm) corresponding to free and lipid-bound TFPP. Furthermore, the solution ^{13}C TFPP NMR resonance at 177 ppm and ^{19}F TFPP solution NMR resonance (Fig. 3) exhibited either splitting into two lines or the appearance of shoulders. While these additional resonances and shoulders were not identified in this proof-of-principle study, we hypothesize that there are possibly more than two (free and lipid-bound) exchange compartments. These could include chemical exchange with additional distribution spaces or compartments like endothelial cell membranes and/or sequestration into intercellular clefts with desmosomal lipoprotein structures.

It is also plausible that a small fraction of hyperpolarized TFPP could interact with enzymes of the plasma or the red and/or white blood cells. For example, the ester group in TFPP could be hydrolyzed by the ubiquitous esterases in the blood. This could explain a drastically different chemical shift of the resonance at 186 ppm, which is within the range of chemical shifts of carboxylic acids in deprotonated form. We expect to assign these additional minor resonances and shoulders in the future.

Limitations

Additional *in vivo* experimental work is necessary to determine the efficacy and specificity of hyperpolarized agents such as TFPP to sense lipids in atheromas and compare with the

published molecular imaging data on LDLR mouse models (19). The experiments described above were performed under conditions in which binding is not in equilibrium with the free tracer. These are all non-steady state, transitional data. It remains to be seen whether the non-steady state analysis combined with appropriate corrections for T_1 changes during the time of exposure will enable the determination of the number of compartments that contribute to the overall signal under the constraints of *in vivo* hyperpolarization conditions. We are currently attempting to model the non-steady state dynamics of hyperpolarized TFPP in *in vivo* situations. Furthermore, the experiments presented here required TFPP to be dissolved in 30% ethanol to achieve adequate delivery to the animal. This is a problem as almost any lipophilic molecule could be potentially solubilized in ethanol and when injected directly into the heart might be expected to localize there. It is not clear if ethanol will inactivate or even precipitate plasma proteins/enzymes or possibly change the permeability characteristics and kinetics of cellular membranes, both within the atheroma as well in the surrounding intact endothelial layers. This shortcoming can be overcome by developing a delivery mechanism devoid of ethanol solvent, using perhaps albumin or other common drug delivery systems. Work is in progress in our laboratory to design, synthesize and test a family of other water soluble molecules that target lipid rich atheroma. Nanoparticular liposomal formulations are also under consideration.

Conclusions

We demonstrated a novel strategy for sensing lipid content on arterial wall *in vivo* by employing ^{13}C hyperpolarized MR. This general strategy may represent a powerful way to target biological receptors for MR imaging and spectroscopy. Since this novel use of ^{13}C hyperpolarization sufficiently generated an MR signal *in vivo*, it may be possible to design hyperpolarized molecules with diverse binding properties like that currently employed in Positron Emission Tomography (PET).

Methods

Hyperpolarization

Parahydrogen addition and transfer of spin order to ^{13}C has been previously described (20, 21). The design and the selection of the reagent has been described elsewhere (13,14). This molecular agent has two important moieties: the lipophilic fluorocarbon motif $-CH_2-CF_2-CF_2H$ and $C{=}C-^{13}C$ functionality for ^{13}C PHIP hyperpolarization. A custom built PHIP polarizer (Huntington Medical Research Institutes (HMRI) (22,23) was employed to hydrogenate the double bond of the acrylate moiety in TFPA to yield 2,2,3,3-tetrafluoropropyl 1-^{13}C-propionate-$d_{2,3,3}$ (TFPP) (Fig. 1a). The spin order was transferred from ^1H nuclei to ^{13}C at 1.76 mT in the reactor by the heteronuclear pulse sequence described by Goldman and Johannesson (21) using the hetero- and homonuclear J coupling of 2-hydroxyethyl 1-^{13}C-propionate-$d_{2,3,3}$ (HEP). The resulting hyperpolarized TFPP product dissolved in aqueous ethanol (30%) was delivered to the 4.7 T MR scanner (Bruker Avance, Bruker AG, Germany) and was detected 25–40 s following production, using a $^1H/^{13}C$ MR solenoid coil and $^1H/^{13}C$ full body mouse volume coil (Doty Scientific, South Carolina, USA) (22).

To quantify the degree of hyperpolarization, we used the reference of a single scan spectrum of thermally polarized natural abundance ethanol at 4.7 T using the following formula:

$$\%P_{t=\text{detection}} = \frac{[\text{reference}]}{[\text{polarized}]} * \frac{\text{signal (polarized)}}{\text{signal (reference)}} * \frac{100\%}{246,600} \quad (1)$$

where 1/246,600 corresponds to ^{13}C nuclear polarization at 298 K and at 4.7 T, according to the Boltzmann distribution. The degree of hyperpolarization produced in the PHIP polarizer at time zero was back calculated, using the delivery time and spin-lattice relaxation time T_1 of the hyperpolarized agent as follows:

$$\%P_{t=0} = \%P_{t=detection} * \exp\left(\frac{\text{delivery time}}{T_1}\right) \quad (2)$$

The reported % hyperpolarization refers to $\%P_{t=0}$.

In vivo experiments in mice

The *in vivo* portion of this study involved non-survival, intracardiac injections of hyperpolarized TFPP into C57BL/6 mice. Three LDLR deficient mice (Jackson Laboratories) were fed a high fat, Western type of diet (Harland Teklad) for nine months. They reached 30–35 g while four normal control mice weighed only 20–25 g after nine months on a regular diet. Necropsy revealed that the LDLR deficient /high fat diet mice acquired atherosclerotic lesions in the aorta and aortic valve. For each scan, a mouse was anesthetized with 1.5% isoflurane gas, 0.8 L/min oxygen per facemask After being placed in a heated volume coil, the 4.7 T Bruker MR scanner was shimmed. The mouse was then taken out of the scanner for laparotomy, which allowed for a transdiaphragmatic intracardiac injection of 1 mL of 11–42 mM TFPP under direct visualization using a 28-gauge needle. The mouse was then quickly re-inserted into the scanner, with care to maintain shim geometry. The time from injection to beginning of scan averaged 15 seconds. After the scan, the mouse was immediately dissected to harvest the portion of aorta that spanned the root to the diaphragm. All animal experiments were approved by IUCAC of HMRI and Burnham Institute. ^{13}C non-localized spectra were acquired either as a single spectrum with large angle excitation pulse or multiple spectra (up to 512 scans as shown in Figs. 3g, 3h and 4) with small angle excitation pulse.

Acknowledgments

We thank the following for funding: Tobacco Related Disease Research Program 16KT-0044 and 16RT-0184, NIH/NCI R01 CA 122513, 1R21 CA118509, 1K99CA134749-01, Rudi Schulte Research Institute, James G. Boswell Fellowship, American Heart Association, American Brain Tumor Association, Prevent Cancer Foundation. We thank Profs. Daniel P. Weitekamp and Peter B. Dervan, Drs. Valerie A. Norton, Keiko Kanamori, Jan Hovener, Napapon Sailasuta, Kent Harris and Siu-Kei Chow for useful discussion.

Abbreviations

DMPC	1,2-dimyristoylphosphatidylcholine
DNP	Dynamic Nuclear Polarization
HEP	Hydroxyethylpropionate
LDLR	Low Density Lipoprotein Receptor
LDL	Low Density Lipoprotein
MR	Magnetic Resonance
MRI	Magnetic Resonance Imaging
MRS	Magnetic Resonance Spectroscopy
NMR	Nuclear Magnetic Resonance

PHIP	Parahydrogen Induced Polarization
TFPA	tetrafluoropropylacrylate
TFPP	tetrafluoropropylpropionate

References

1. Hove MT, Neubauer S. Evaluating metabolic changes in heart disease by magnetic resonance spectroscopy. Heart Metab. 2006; 32:18–21.
2. Abragam A, Goldman M. Principles of Dynamic Nuclear-Polarization. Rep. Prog. Phys. 1978; 41:395–467.
3. Bowers CR, Weitekamp DP. Transformation of Symmetrization Order to Nuclear-Spin Magnetization by Chemical-Reaction and Nuclear-Magnetic-Resonance. Phys. Rev. Lett. 1986; 57:2645–2648. [PubMed: 10033824]
4. Bowers CR, Weitekamp DP. Para-Hydrogen and Synthesis Allow Dramatically Enhanced Nuclear Alignment. J. Am. Chem. Soc. 1987; 109:5541–5542.
5. Ardenkjaer-Larsen JH, Fridlund B, Gram A, Hansson G, Hansson L, Lerche MH, Servin R, Thaning M, Golman K. Increase in signal-to-noise ratio of > 10,000 times in liquid-state NMR. Proc Natl Acad Sci U S A. 2003; 100:10158–10163. [PubMed: 12930897]
6. Golman K, in't Zandt R, Thaning M. Real-time metabolic imaging. Proc Natl Acad Sci U S A. 2006; 103:11270–11275. [PubMed: 16837573]
7. Golman K, in't Zandt R, Lerche M, Pehrson R, Ardenkjaer-Larsen JH. Metabolic imaging by hyperpolarized 13C magnetic resonance imaging for in vivo tumor diagnosis. Cancer Res. 2006; 66:10855–10860. [PubMed: 17108122]
8. Day SE, Kettunen MI, Gallagher FA, Hu DE, Lerche M, Wolber J, Golman K, Ardenkjaer-Larsen JH, Brindle KM. Detecting tumor response to treatment using hyperpolarized (13)C magnetic resonance imaging and spectroscopy. Nat. Med. 2007; 13:1382–1387. [PubMed: 17965722]
9. Gallagher FA, Kettunen MI, Day SE, Hu DE, Ardenkjaer-Larsen JH, in't Zandt R, Jensen PR, Karlsson M, Golman K, Lerche MH, Brindle KM. Magnetic resonance imaging of pH in vivo using hyperpolarized 13C-labelled bicarbonate. Nat. 2008; 453:940–943.
10. Bhattacharya P, Chekmenev EY, Perman WH, Harris KC, Lin AP, Norton VA, Tan CT, Ross BD, Weitekamp DP. Towards hyperpolarized (13)C-succinate imaging of brain cancer. J. Magn. Reson. 2007; 186:150–155. [PubMed: 17303454]
11. Chekmenev EY, Hovener J, Norton VA, Harris K, Batchelder LS, Bhattacharya P, Ross BD, Weitekamp DP. PASADENA hyperpolarization of succinic acid for MRI and NMR spectroscopy. J. Am. Chem. Soc. 2008; 130:4212–4213. [PubMed: 18335934]
12. Bhattacharya P, Harris K, Lin AP, Mansson M, Norton VA, Perman WH, Weitekamp DP, Ross BD. Ultra-fast three dimensional imaging of hyperpolarized C-13 in vivo. Magn. Reson. Mat. Phys. Biol. Med. 2005; 18:245–256.
13. Bhattacharya P, Ross BD, Bunger R. Cardiovascular applications of hyperpolarized contrast media and metabolic tracers. Exp. Biol. Med. 2009; 234:1395–1416.
14. Chekmenev EY, Chow SK, Tofan D, Weitekamp DP, Ross BD, Bhattacharya P. Fluorine-19 NMR chemical shift probes molecular binding to lipid membranes. J. Phys. Chem. B. 2008; 112:6285–6287. [PubMed: 18422359]
15. Choudhury RP, Fuster V, Fayad ZA. Molecular, cellular and functional imaging of atherothrombosis. Nat. Rev. Drug Discov. 2004; 3:913. [PubMed: 15520814]
16. Lipinski MJ, Amirbekian V, Frias JC, Aguinaldo JGS, Mani V, Briley-Saebo KC, Fuster V, Fallon JT, Fisher EA, Fayad ZA. MRI to detect atherosclerosis with gadolinium-containing immunomicelles targeting the macrophage scavenger receptor. Magn. Reson. Med. 2006; 56:601–610. [PubMed: 16902977]
17. Moore KJ, Freeman MW. Scavenger Receptors in Atherosclerosis Beyond Lipid Uptake. Arteriosclerosis Thrombosis and Vascular Biology. 2006; 26:1702–1711.

18. Castellani LW, Chang JJ, Wang XP, Lusis AJ, Reynolds WF. Transgenic mice express human MPO 2463G/A alleles at atherosclerotic lesions, developing hyperlipidemia and obesity in 2463G males. J. Lipid Res. 2006; 47:1366–1377. [PubMed: 16639078]

19. Li D, Patel AR, Klibanov AL, Kramer CM, Ruiz M, Kang BY, Mehta JL, Beller GA, Glover DK, Meyer CH. Molecular Imaging of Atherosclerotic Plaques Targeted to Oxidized LDL Receptor LOX-1 Using SPECT/CT and Magnetic Resonance. Circ. Cardiovasc. Imag. 2010; 3:464–472.

20. Johannesson H, Axelsson O, Karlsson M. Transfer of para-hydrogen spin order into polarization by diabatic field cycling. C. R. Physique. 2004; 5:315–324.

12. Goldman M, Johannesson H. Conversion of a proton pair para order into ^{13}C polarization by rf irradiation, for use in MRI. C. R. Physique. 2005; 6:575–581.

22. Hövener JB, Chekmenev E, Harris K, Perman W, Robertson L, Ross BD, Bhattacharya P. PASADENA hyperpolarization of 13C biomolecules: equipment design and installation. Magn. Reson. Mat. Phys. Biol. Med. 2009; 22:111–121.

23. Hövener JB, Chekmenev E, Harris K, Perman W, Tran T, Ross BD, Bhattacharya P. Quality assurance of PASADENA hyperpolarization for 13C biomolecules. Magn. Reson. Mat. Phys. Biol. Med. 2009; 22:123–134.

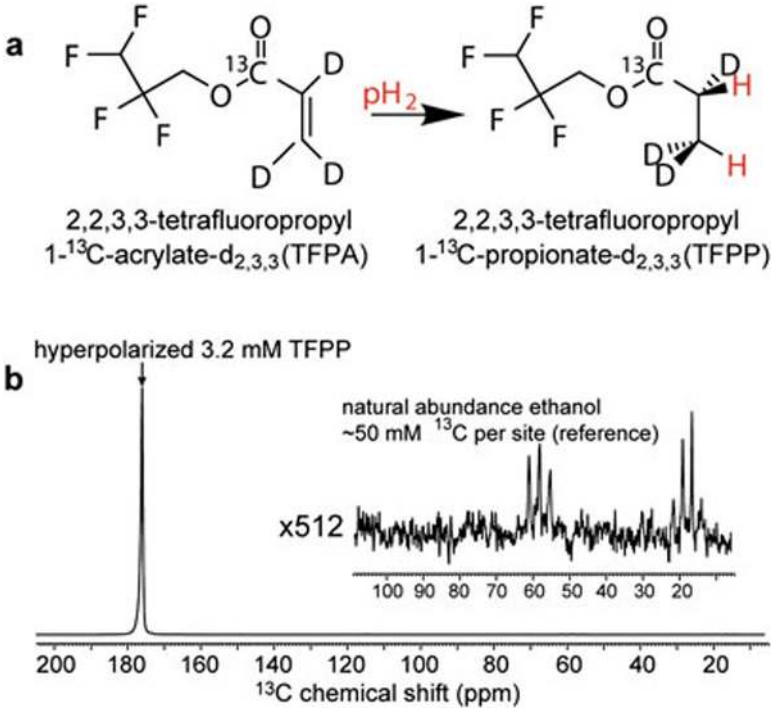

Figure 1.

a) Molecular cis addition of parahydrogen to TFPA to produce TFPP. The catalytic reaction was carried out at 62°C but the hyperpolarized solution was cooled to 35–40°C by the time it comes out of the polarizer. b) Quantification of PHIP ^{13}C signal enhancement by ^{13}C spectroscopy of hyperpolarized 3.2 mM TFPP at 4.7 T *in vitro*. Polarization of 17% was achieved in this representative example. The inset spectrum shows a reference signal obtained from the natural abundance 4.5 M ethanol, ^{13}C concentration = 50 mM per carbon site.

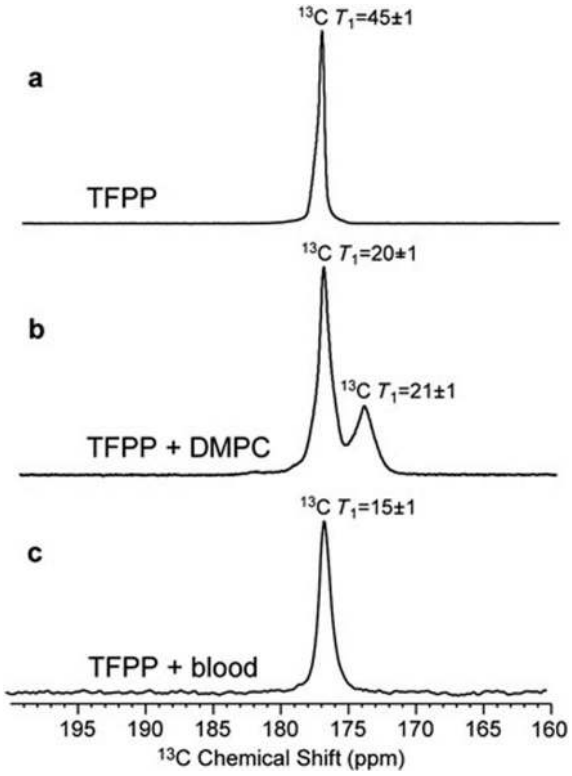

Figure 2.

^{13}C hyperpolarized spectra of TFPP in aqueous solutions acquired with 10° excitation pulse at 35–40°C: a) 6 mM TFPP, 4.5 M ethanol (EtOH), b) 2 mM TFPP, 1.5 M EtOH, 20 mM DMPC, c) 2 mM TFPP, 1.8 M EtOH in 60% porcine blood. ^{13}C T_1 value shown for each resonance was measured by recording ^{13}C hyperpolarized signal decay with small angle excitation pulses.

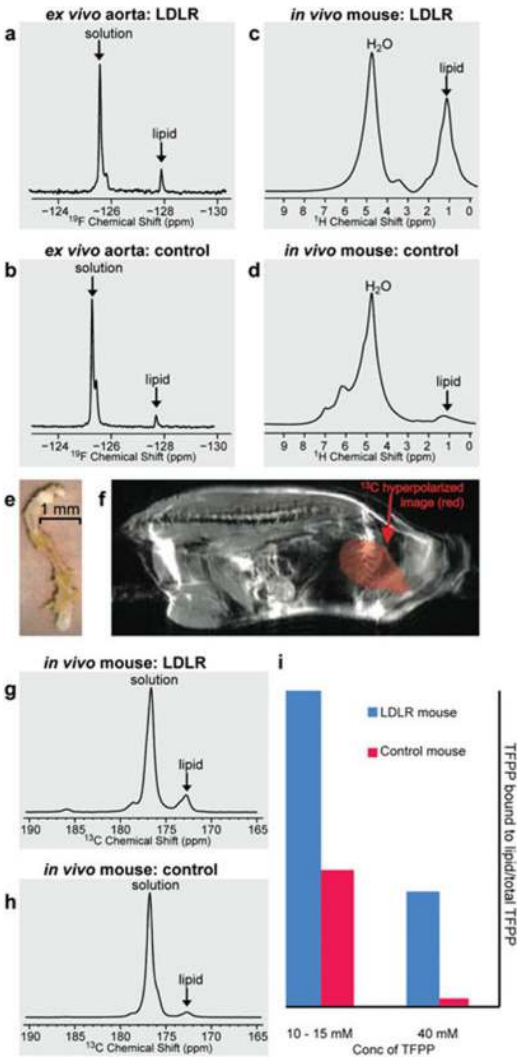

Figure 3.

^{19}F *ex vivo* NMR spectra of LDLR (a) and control (b) mouse aorta demonstrating lipid binding of TFPP from 30% EtOH aqueous solution. Spectra recorded using Magic Angle Spinning (MAS) at 6–10 kHz without proton decoupling at 11.7 T. *In vivo* non-localized ^{1}H spectra acquired in LDLR (c) and control (d) mice confirm excess lipid in LDLR mice. (e) the photograph of harvested aorta. (f) proton image, RARE factor 4, 2 averages, 0.3 mm × 0.3 mm in plane resolution, 9 min acquisition provides the anatomical location, where proton spectra were acquired. *In vivo* ^{13}C PHIP hyperpolarized non-localized NMR spectra acquired after 1 mL 13 mM TFPP intracardiac injection in LDLR, animal #2, (g) and control, animal #4 (h) mice. 512 spectra (0.178 s each) were acquired with 10° excitation pulse for each animal during 76 s acquisition time course. The average of 64 individual scans acquired in 9.5 s is shown in Figs. 3g and 3h. The detailed time course is provided in Figure 4. In a separate experiment, fast ^{13}C image, 2D FISP sequence 3 mm ×3 mm resolution, 1 average, 30° flip angle, 0.12 s acquisition, shown as a red overlay over proton image in Fig. 3e was acquired prior to hyperpolarized ^{13}C spectroscopy acquisition. ^{13}C and ^{1}H *in vivo* spectra are acquired using ^{1}H/^{13}C double-tuned volume coil at 4.7 T. (i) the distribution of the *in vivo* hyperpolarized ^{13}C signal (hyperpolarized lipid TFPP): (hyperpolarized total TFPP) in LDLR (blue) and control (red) mice under two different concentrations of injected hyperpolarized substrate.

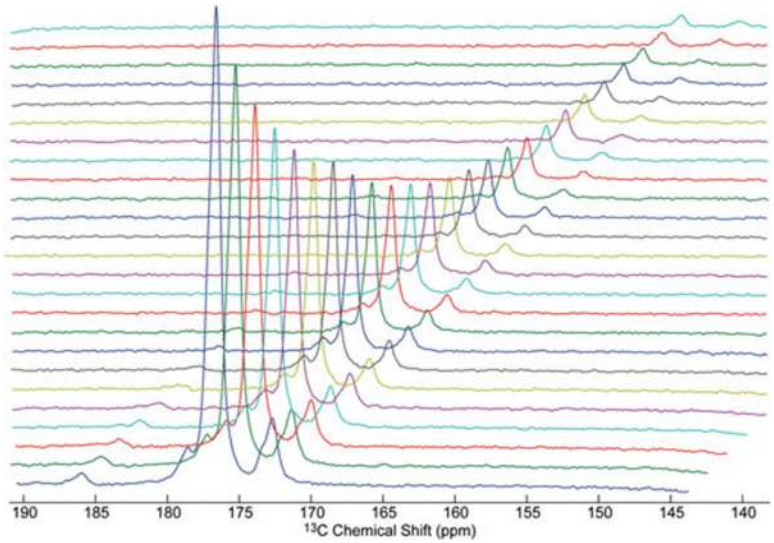

Figure 4.

In vivo time course of ^{13}C hyperpolarized TFPP signal decay after intracardiac injection of 1mL 13 mM TFPP in a LDLR mouse corresponding to Fig. 3D. Each spectrum (temporal resolution is 1.78 s) is an average of 12 individual scans acquired using $^{1}H/^{13}C$ double resonance volume coil (Doty Scientific, South Carolina, USA) at 4.7 T. Acquisition parameters: excitation pulse = 10°, spectral width=4,000 Hz, acquisition time=128 ms, repetition time = 148 ms. MR scan # 1 (first) and #300 (last) were recorded 15 s and 60 s after injection respectively.